



Deposited via The University of Leeds.

White Rose Research Online URL for this paper:

<https://eprints.whiterose.ac.uk/id/eprint/133934/>

Version: Accepted Version

---

**Proceedings Paper:**

Chen, L, Figueredo, LFC and Dogar, M (2019) Manipulation Planning Under Changing External Forces. In: Proceedings of the IEEE/RSJ International Conference on Intelligent Robots and Systems (IROS 2018). IROS 2018: IEEE/RSJ International Conference on Intelligent Robots and Systems, 01-05 Oct 2018, Madrid, Spain. IEEE, pp. 3503-3510. ISBN: 978-1-5386-8094-0. ISSN: 2153-0866. EISSN: 2153-0866.

<https://doi.org/10.1109/IROS.2018.8593555>

---

© 2018 IEEE. This is an author produced version of a paper published in Proceedings of the IEEE/RSJ International Conference on Intelligent Robots and Systems (IROS 2018). Personal use of this material is permitted. Permission from IEEE must be obtained for all other uses, in any current or future media, including reprinting/republishing this material for advertising or promotional purposes, creating new collective works, for resale or redistribution to servers or lists, or reuse of any copyrighted component of this work in other works. Uploaded in accordance with the publisher's self-archiving policy.

**Reuse**

Items deposited in White Rose Research Online are protected by copyright, with all rights reserved unless indicated otherwise. They may be downloaded and/or printed for private study, or other acts as permitted by national copyright laws. The publisher or other rights holders may allow further reproduction and re-use of the full text version. This is indicated by the licence information on the White Rose Research Online record for the item.

**Takedown**

If you consider content in White Rose Research Online to be in breach of UK law, please notify us by emailing [eprints@whiterose.ac.uk](mailto:eprints@whiterose.ac.uk) including the URL of the record and the reason for the withdrawal request.

# Manipulation Planning under Changing External Forces

Lipeng Chen, Luis F. C. Figueredo, Mehmet Dogar

**Abstract**—We present a manipulation planning algorithm for a robot to keep an object stable under changing external forces. We particularly focus on the case where a human may be applying forceful operations, e.g. cutting or drilling, on an object that the robot is holding. The planner produces an efficient plan by intelligently deciding when the robot should change its grasp on the object as the human applies the forces. The planner also tries to choose subsequent grasps such that they will minimize the number of regrasps that will be required in the long-term. Furthermore, as it switches from one grasp to the other, the planner solves the problem of bimanual regrasp planning, where the object is not placed on a support surface, but instead it is held by a single gripper until the second gripper moves to a new position on the object. This requires the planner to also reason about the stability of the object under gravity. We provide an implementation on a bimanual robot and present experiments to show the performance of our planner.

## I. INTRODUCTION

We are interested in the problem of a robot manipulating an object that is under the application of changing external forces. Take the example in Fig. 1, where a human is cutting a circular piece out of a board. During the cutting operation, the human exerts forces on the board that change position, direction, and magnitude. To keep the object stable against these forces, the robot changes its grasp on the object multiple times. In this paper we propose a planner that enables a robot to keep an object stable under changing external forces like this.

There are two key problems our planner solves.

First, our planner produces an efficient plan by minimizing the number of times the robot needs to regrasp the object. For example in Fig. 1, the robot changes its grippers' position only 2 times (counting each gripper separately) during the whole operation. This requires the planner to decide **when** to regrasp during the course of the interaction. It also requires the planner to choose grasps intelligently. A bad grasp may result in failure; for example the object may slip through the fingers during a cutting action (Fig. 2(a)), or it may bend away from the desired pose due to large torques around the gripper during a drilling action (Fig. 2(b)).

Second, our planner plans each regrasp. A regrasp requires the robot to release its grippers off the object and then to grasp the object at different points. However, when the robot releases a gripper, the object may become unstable under external forces. Even if we assume the human in Fig. 1(a)

This project has received funding from the European Union's Horizon 2020 research and innovation programme under the Marie Skłodowska-Curie grants agreement No. 746143 and 795714, and from the UK Engineering and Physical Sciences Research Council under grant EP/P019560/1.

Authors are with School of Computing, University of Leeds, Leeds, UK, {s1c1, l.figueredo, m.r.dogar}@leeds.ac.uk

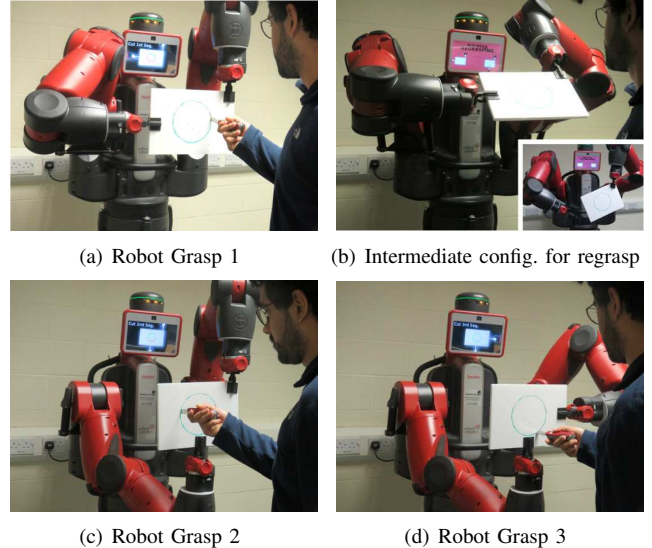


Fig. 1. Cutting a circular piece out of a board.

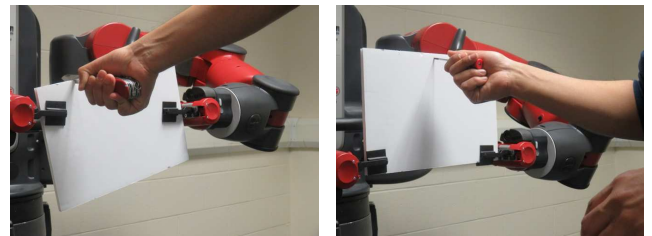


Fig. 2. Failure during cutting (a) and drilling (b).

stops applying forces during regrasps, the object can still become unstable due to gravity. For example, to regrasp the object from the configuration in Fig. 1(a) to the one in Fig. 1(c), if the robot simply releases its right gripper, a heavy object may slip within the remaining gripper as shown in the small figure at the right bottom of Fig. 1(b). Therefore, the robot may need to change the position of the object before releasing one of its grippers. Fig. 1(b) shows such an intermediate pose, where the object is stable even when the right gripper releases it.

In a typical *multi-step manipulation planning* problem [1], a robot moves an object through geometric obstacles where the robot ungrasps and regrasps the object multiple times. The need to regrasp objects was recognized even in the earliest manipulation systems [2], [3]. More recently, planners have been proposed to solve the regrasp planning

problem in the case of multiple manipulators for assembly-like tasks [4], [5], [6], [7].

We build on and extend this literature in three novel ways.

First, in addition to the kinematic and geometric (e.g. collision) constraints, we also consider stability constraints due to the changing external forces acting on the manipulated object. Multi-step manipulation planners need to go beyond geometric constraints. In our task, for example, the robot is not required to move the object to any goal position but is simply required to keep the object stable. Still, due to the sequence of external forces acting on the object, the robot needs to plan regrasps and the corresponding motions, possibly moving the object as a result. In this paper we present such a manipulation planner. Similar to Bretl [8] we formulate the problem as first identifying the stable intersections between different grasp manifolds and then connecting these intersections.

Second, we solve the problem of regrasp planning “in-the-air” using two manipulators. Existing work in regrasp planning focuses on placing an object on a support surface and then regrasping it with a new gripper pose [5], [6], [7]. In our task, the robot performs the regrasp without placing the object on a surface. Instead, it goes through a sequence of unimanual and bimanual grasps to reach different grasps. This, however, requires our planner to also evaluate the stability of the object against gravity, particularly during unimanual grasps.

Third, we are interested in addressing multi-step manipulation planning in a *human-robot interaction* setting. Therefore we strive to minimize the number of different grasps required to hold the object stable against external forces. We also have constraints in terms of where we position the object in space to make it possible for the human to apply the forces. Existing work in forceful human-robot collaboration mostly focuses on the control problem [9], [10], [11], solving for the necessary stiffness of manipulator joints as an external force is applied, and assumes the object to be already grasped at pre-specified points by the robot. We approach the problem from the manipulation planning point of view and instead address the decision of what grasps to use and when/how to switch between them. Other work in planning for human-robot collaboration exists [12], [13], [14] which focus on handing-over an object to a human, or avoiding colliding a human working in the same workspace. To the best of our knowledge our work is the first one to take a planning approach to the human-robot collaboration problem where the human applies multiple changing forces on an object grasped by the robot.

## II. PROBLEM DEFINITION

In this paper, we are interested in scenarios where forces are exerted on the object grasped by the robot. We use  $f$  to refer to a force vector, defined in the object’s coordinate frame. Then, we represent a forceful task to be executed on the object as a sequence of forces  $F = (f_i)_{i=1}^m$ . For example, in Fig. 3-Left, a sequence of sixteen force vectors tangential to the circle represent the circular cutting task in Fig. 3.

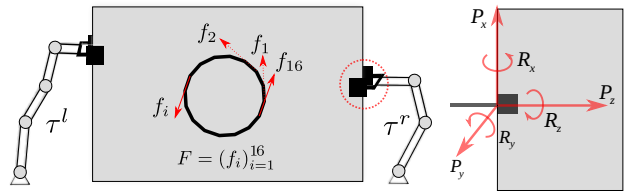


Fig. 3. Left: The task is represented as a sequence of forces  $F = (f_i)_{i=1}^m$ . Right: We estimate the force/torque limits of a grip on the object along the three main axes.

Here, we assume the robot has two manipulators for clarity of explanation and because the robot we use in our experiments has two arms. However, our formulation can easily be extended to more manipulators. We assume each manipulator is equipped with a gripper. Let  $CS^l$ ,  $CS^r$  be the configuration space of the left and right manipulator, and  $SE(3)$  be the configuration space of the object. The composite configuration space  $CS$  is their Cartesian product  $CS = CS^l \times CS^r \times SE(3)$ . Each composite configuration  $q$  in  $CS$  can then be written as  $q = (q^l, q^r, x)$ , where  $q^l \in CS^l$ ,  $q^r \in CS^r$ , and  $x \in SE(3)$ .

We also define a *grasp*,  $g$ , using the pose of the gripper(s) on the object. A bimanual grasp specifies poses for both the left and right grippers. A unimanual grasp specifies the pose of only one gripper. Such gripper poses can be generated using a grasp planner, e.g. Miller and Allen [15]. For example, the parallel plate grippers of the Baxter robot, which we use in this work, can grip any point on the edges of the board.

A configuration  $q$  and a grasp  $g$  are related via forward/inverse kinematics. Furthermore, the configuration space  $CS$  consists of a collection of lower-dimensional manifolds, where each manifold corresponds to a particular unimanual or bimanual grasp of the object. We use  $M(g)$  to refer to the manifold for grasp  $g$ . For our planner, changing the grasp on the object means changing the manifold the system is in.

In this paper, the robot’s task is to stably grasp the object during the application of forces. Given a single force  $f$ , we can check whether the system is stable at a configuration  $q$ , using formulations from the literature in grasp stability and cooperative manipulation (We explain how we perform this check in Sec. III-A.1). However, to reduce the number of regrasps required, the robot can use one configuration against multiple external forces in a row. In this work, we say that a configuration  $q$  is **stable against** a sequence of forces  $(f_i)_{i=1}^m$  if, at  $q$ , the system is stable against all  $f_i$ . Moreover, we say that a sequence of configurations  $Q = (q_i)_{i=1}^p$  is stable against a sequence of forces  $F = (f_i)_{i=1}^m$ , if the configurations in  $Q$  cover all the forces in  $F$  in order, i.e. if  $q_1$  is stable against  $(f_1, \dots, f_j)$ , and  $q_2$  is stable against  $(f_{j+1}, \dots, f_k)$ , and so on until  $q_p$  is stable against  $(f_{n+1}, \dots, f_m)$ , where  $1 \leq j < k \leq n < m$ . For example the three configurations shown in Fig. 1 are stable against the forces distributed along a circle as shown in Fig. 3. Notice that different configurations correspond to different grasps on the object.

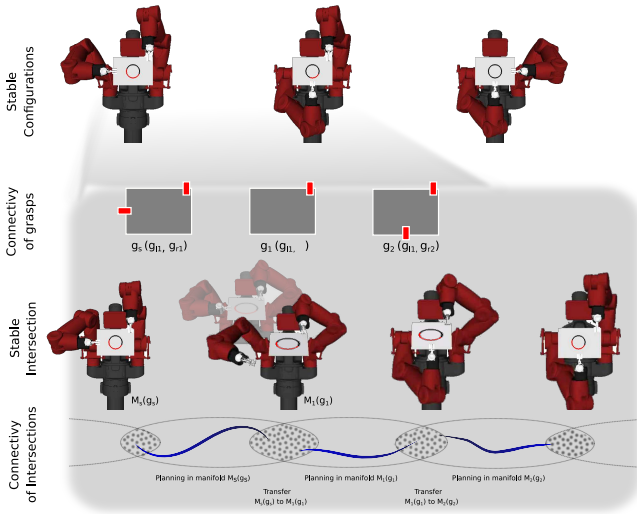


Fig. 4. Overview of approach.

Finding a small set of configurations  $Q = (q_i)_{i=1}^p$  to resist the forces is only part of the problem. The robot must also be able to move between these configurations, using collision-free and stable trajectories.

Therefore, given a sequence of external forces  $F = (f_i)_{i=1}^m$  and a starting configuration of the system  $q_0$ , we define the problem of **manipulation planning under changing external forces** as the generation of a sequence of configurations  $Q = (q_i)_{i=1}^p$  and a sequence of trajectories  $T = (t_i)_{i=1}^p$ , such that  $Q$  is stable against  $F$  and each trajectory  $t_i$  moves the system from  $q_{i-1}$  to  $q_i$ , is collision-free and is stable against gravity. A trajectory  $t_i$  usually corresponds to a *re-grasping* task.

Furthermore, we are interested in a human-robot interaction scenario. To make this interaction fluent for the human, we have the goal of minimizing the number of regrasps required in the manipulation plan.

In the human-robot interaction setting, we also assume a fixed desired pose of the object,  $x \in SE(3)$ , that is comfortable for the human as he/she applies forces on the object. Therefore, we have the constraint that the configurations  $Q$  in the manipulation plan must position the object at  $x$ .

Hence, a planning query for us is a triple  $(F, q_0, x)$  where  $F$  is the sequence of external forces to be applied on the object,  $q_0$  is the starting configuration of the system, and  $x$  is the desired pose of the object when the forces  $F$  are applied.

#### A. Overview of approach

Our problem is an instance of *multi-modal planning* [16], [8], [17], where each different modality corresponds to a different bimanual or unimanual grasp. In developing a planner, we follow a similar strategy of first identifying intersection points between different modalities/manifolds, and then planning motion paths to connect them. We illustrate our overall planning approach in Fig. 4 in four layers. We present the details of each layer in Sec. III. Here we present a brief overview and explain how these layers fit together:

- *Generating configurations stable against  $F$ .* Given  $F$  and  $x$ , we first identify a candidate  $Q = (q_i)_{i=1}^p$  which is stable against  $F$ , while minimizing the number of regrasps.  $Q$  also positions the object at  $x$ . The three robot-object configurations shown in the top layer in Fig. 4 is an example output. Given  $Q$ , the lower layers of the planner try to connect each subsequent configuration in  $Q$ .
- *Connectivity of grasps.* Given two subsequent configurations generated in the top layer,  $q_i$  and  $q_{i+1}$ , we identify a sequence of grasps  $G = (g_j)_{j=1}^n$  on the object to move the grippers from their positions in  $q_i$  to their positions in  $q_{i+1}$ . The second layer in Fig. 4 shows an example grasp sequence, connecting the grasps in the first two configurations of the top layer. Note that there are many other possible contact sequences here, possibly going through other intermediate gripper contacts as shown in Fig. 5(c).
- *Sampling stable intersections of grasp manifolds.* Given two subsequent grasps  $g_i$  and  $g_{i+1}$  from the sequence generated in the layer above, we sample a set of candidate configurations at which the transition from  $g_i$  to  $g_{i+1}$  can be performed stably. The configuration in the middle on the third layer of the Fig. 4 is an example. At the shown configuration, both the unimanual grasp and the bimanual grasp can hold the object stable against gravity, and therefore this configuration is a good candidate to change between two grasp manifolds.
- *Connectivity of manifold intersections.* Given a set of configurations at the intersections of sequences of grasp manifolds, this fourth layer performs collision-free and stability-constrained motion planning within the manifolds to connect the configurations.

The layered structure of our planner enables us to minimize the number of regrasps at the top layer, but leaves the time-consuming motion planning to the final layer, enabling fast planning time.

### III. APPROACH

In this section we describe the details of our planner.

#### A. Generating configurations stable against $F$

Our planner takes input the sequence of forces  $F$  and the desired object pose  $x$ . It starts by generating a sequence of configurations  $Q$  such that  $Q$  is stable against  $F$ , the configurations in  $Q$  position the object at  $x$ , and the number of regrasps between the configurations in  $Q$  is minimized.

Given an external force  $f$ , we can identify a set of configurations in  $CS$  which are stable against this force. In Fig. 5(a), the red, green and blue regions illustrate such sets for forces  $f_1$ ,  $f_2$ , and  $f_i$  respectively. Note that there might be intersections between these stable regions, and a configuration in the intersections is stable against multiple forces; e.g. configuration  $q_2$  in the figure is stable against both  $f_1$  and  $f_2$ .

Then our problem is to find a sequence  $Q = (q_i)_{i=1}^p$  such that the configurations visit the regions for each  $f_i \in F$  in

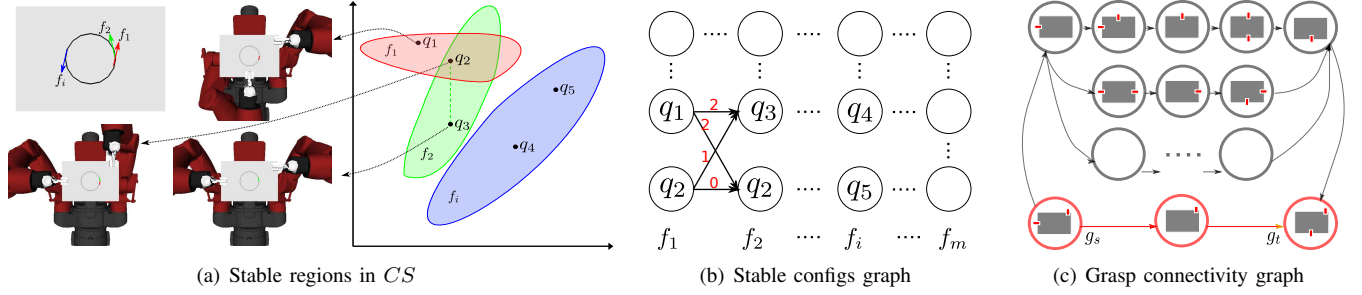


Fig. 5. (a) and (b): Planning stable configurations. (c) Planning grasp connectivity.

order. Moreover, we are interested in identifying a sequence  $Q$ , such that it will minimize the needs for regrasping.

To create such a sequence of configurations  $Q$ , we first sample a set of candidate configurations in  $CS$ . To sample configurations that are likely to be stable against a variety of forces, we start by sampling grasps on the object. Using such a sampled grasp  $g$  and the desired object position  $x$ , we solve the inverse-kinematics problem, which may have many solutions, and sample a single configuration  $q$ .

For each sample  $q$ , we identify the forces in  $F$  that  $q$  is stable against (Details of the stability check is explained below in Sec. III-A.1). We then build a directed weighted graph using these configurations as shown in Fig. 5(b). In the graph, the nodes in the  $i^{\text{th}}$  column are the sampled configurations that are stable against force  $f_i$ . Then we create a link from every node in  $i^{\text{th}}$  column to every node in  $(i+1)^{\text{th}}$  column. We associate each link with a weight using the number of gripper moves required from one configuration to the other. For example, the weight between the node  $q_2$  in the first column and the node  $q_2$  in the second column is zero, since the two nodes are the same configurations and no re-grasping is needed. Similarly, if two configurations differ only by one gripper location on the object, the weight for the link between them is set as one. Otherwise, the weight would be two. Note that one can come up with other weighting schemes, e.g., one that takes into account the distance between grasp points.

At this point, our problem in this layer can be formulated as graph search. We want a path that starts from one node in the leftmost column for  $f_1$  and ends with a node in the rightmost column for  $f_m$ . We can search the graph for an optimal path. We use *Dijkstra's algorithm*, which gives us the sequence  $Q$  with the least number of gripper moves based on the current set of samples. We call this planner the *min-regrasp* planner.

Building the graph requires knowing the sequence of external forces  $F$  beforehand. If the forces are revealed one by one, then the graph can be formed as the next force is specified, and it can be searched greedily. We call this version the *greedy planner*.

We provide the pseudo-code for this layer of our planner in Alg. 1 in the procedure *PlanStableSequence*. On line 1, we generate the graph as described above. On line 2, we search this graph (e.g., Dijkstra's) to generate  $Q$ . Then we iterate over every subsequent pair of configurations in  $Q$  (line 4), and try to plan a regrasp between them, which is

explained below. If the regrasp planning fails between two configurations (line 6), we remove the failing link from the graph in Fig. 5(b) (line 7), and re-search the graph to generate a new  $Q$  (line 8).

---

#### Algorithm 1 Manipulation planning under changing forces

---

```

PlanStableSequence ( $F, q_0, x$ ):
1:  $V, E \leftarrow$  Sample configs and build graph in Fig. 5(b)
2:  $Q \leftarrow \text{GraphSearch}(V, E)$ 
3:  $Q \leftarrow$  Append  $q_0$  to beginning of  $Q$ 
4: for each subsequent  $q_{i-1}$  and  $q_i$  in  $Q = (q_i)_{i=1}^p$  do
5:    $t_i \leftarrow \text{PlanRegrasp}(q_{i-1}, q_i)$ 
6:   if PlanRegrasp failed then
7:      $V, E \leftarrow$  Remove failing edge from graph  $V, E$ 
8:     Go to line 2
9: return ( $Q = (q_i)_{i=1}^p, T = (t_i)_{i=1}^p$ )

PlanRegrasp ( $q_s, q_t$ ):
1:  $V, E \leftarrow$  Sample grasps and build graph in Fig. 5(c)
2:  $G \leftarrow \text{GraphSearch}(V, E)$ 
3:  $t \leftarrow \text{Connect}(q_s, G = (g_i)_{i=1}^n, q_t)$ 
4: if Connect failed then
5:   if maximum number of attempts reached then
6:     return failure
7:    $V, E \leftarrow$  Remove failing edge from graph  $V, E$ 
8:   Go to line 2
9: else
10:  return  $t$ 

SampleIntersection ( $g, g'$ ):
1: One of  $g$  and  $g'$  must be bimanual. Assuming  $g$ .
2:  $S \leftarrow \{\}$ 
3: while  $S$  has less than  $m$  samples do
4:    $x \leftarrow$  Sample pose for object
5:    $q \leftarrow$  Solve IK with object at  $x$  and grippers at  $g$ 
6:   if  $q$  is stable against gravity with both  $g$  and  $g'$  then
7:     Add  $q$  to  $S$ 
8: return  $S$ 

Connect ( $q_s, G = (g_1, g_2, \dots, g_n), q_t$ ):
1: if  $n = 1$  then
2:    $t \leftarrow \text{MotionPlan}(q_s, q_t)$  using grasp  $g_n$ 
3:   if MotionPlan successful then
4:     return  $t$ 
5:   else
6:     return failure
7:  $S \leftarrow \text{SampleIntersection}(g_1, g_2)$ 
8: for each  $q$  in  $S$  do
9:    $t \leftarrow \text{MotionPlan}(q_s, q)$  using grasp  $g_1$ 
10:  if MotionPlan successful then
11:    return  $t + \text{Connect}(q, G = (g_2, \dots, g_n), q_t)$ 
12: return failure

```

---

1) *Stability check*: Given an external force  $f$ , a configuration of the robot-object system  $q$ , and the gripper contacts on the object, we check the stability of the system against  $f$ . Given an external force on an object grasped by two cooperating manipulators, the *cooperative manipulation* literature provides formulations to compute possible torque distributions on the manipulators' joints. Particularly, Uchiyama et al. provide the symmetric formulation [18], [19], which describes the kinematic and static relationship between the force applied on the object and its counterparts required at the manipulator joints to resist it. This formulation, however, leaves the forces at the grip points unconstrained. In addition to the manipulator joint torque limits, we are also interested in checking whether the grip forces, e.g. the frictional forces between fingers, will be able to resist the external force. This requires the computation of the *grasp wrench space* [20], which is the space of all external wrenches a grasp on an object can stably resist. For the parallel plate grippers we use in this work, we approximate the grasp wrench space with an axis-aligned box in the six-dimensional force-torque space, i.e. as maximum force and torque limits along each of the three main axes around a grip point as shown in Fig. 3-Right, where  $[P_x, P_y, P_z, R_x, R_y, R_z]$  are these estimated limits.

Imposing this additional constraint onto the symmetric formulation of Uchiyama et al. [18], [19], we have the problem:

$$\begin{aligned} J^T f^g &= \tau \\ W f^g &= -f \\ |\tau| &\leq \tau_{\max} \\ |f^g| &\leq f_{\max}^g \end{aligned} \quad (1)$$

where

$$\begin{aligned} J &= \begin{bmatrix} J^l & 0 \\ 0 & J^r \end{bmatrix}, f^g = \begin{bmatrix} f^{g^l} \\ f^{g^r} \end{bmatrix}, \tau = \begin{bmatrix} \tau^l \\ \tau^r \end{bmatrix}, \\ \tau_{\max} &= \begin{bmatrix} \tau_{\max}^l \\ \tau_{\max}^r \end{bmatrix}, f_{\max}^g = \begin{bmatrix} f_{\max}^{g^l} \\ f_{\max}^{g^r} \end{bmatrix} \end{aligned}$$

and

- $J^l$  and  $J^r$  are the Jacobians of the two manipulators at the configuration we are checking the stability;
- $f^{g^l}$  and  $f^{g^r}$  are the forces and torques at the grippers of the two manipulators;
- $\tau^l$  and  $\tau^r$  are the vectors of torques acting at the joints of two manipulators;
- $W$  (sometimes termed the grasp matrix [20], [21], [22]) is a  $(6 \times 12)$  matrix mapping the forces and torques at the grippers to a resultant force on the object;
- $f$  is the external force/torque vector on the object;
- $\tau_{\max}^l$  and  $\tau_{\max}^r$  are the torque limits at the joints of the manipulators;
- $f_{\max}^{g^l}$  and  $f_{\max}^{g^r}$  are our estimates of the maximum force and torque limits along each of the three main axes of each gripper (i.e. our estimate of the grasp wrench space):  $f_{\max}^{g^l} = f_{\max}^{g^r} = [P_x, P_y, P_z, R_x, R_y, R_z]$ .

Eq. 1 is a linear programming problem, and can be solved, e.g. using the Simplex method, to see if there are any feasible solutions of the torques at the joints  $\tau$  and forces/torques at

the grip points  $f^g$ . If this fails, we consider the configuration unstable against the external force.

## B. Connectivity of grasps

Given two subsequent configurations generated in the previous layer,  $q_i$  and  $q_{i+1}$  in  $Q$ , and their corresponding grasps  $g_s$  and  $g_t$ , we identify a sequence of grasps  $G = (g_j)_{j=1}^n$  on the object to move the grippers from  $g_s$  to  $g_t$ . For example, take the first two configurations in the top row of Fig. 4. The robot must go through a number of intermediate grasps to move between the two grasps on the object (These intermediate grasps serve as alternative to the placement of the object on a support surface, which is the dominant approach used for regrasp planning in the literature).

We start by generating a set of unimanual grasps including the gripper positions in  $g_s$  and  $g_t$  and other randomly sampled gripper positions. We then combine these uni-manual grasps to also generate bimanual grasps. Fig. 5(c) represents the connectivity of these grasps as a *grasp graph*. Each node in the graph is a bimanual or uni-manual grasp. A bimanual and a unimanual grasp is connected if the unimanual grasp is one of the gripper poses in the bimanual grasp. Then, the planner can explore the graph to find a possible path from  $g_s$  to  $g_t$ , giving us the required sequence  $G = (g_j)_{j=1}^n$ . This sequence consists of alternating bimanual and unimanual grasps. Fig. 5(c) highlights in red the shortest grasp sequence. There are other longer grasp sequences to connect  $g_s$  and  $g_t$  as well.

The grasp sequence acts as an abstract plan to guide the search in the lower layers of the planner, and contracts the planning into a concrete and finite group of grasp manifolds. In Alg. 1, the procedure *PlanRegrasp* outlines this process. On lines 1-2, we build the grasp graph and search it to generate the sequence of grasps  $G$  as outlined above. We then try to plan the motion from  $q_s$  to  $q_t$  through the grasps  $G$  (line 3). If lower layers of our planner return with a failure to connect two grasps  $g_j$  and  $g_{j+1}$  in  $G$  (line 4), then we remove the link between these grasps in the grasp graph (line 7), and perform the search again to generate a new sequence of grasps (line 8). If the connection is successful, we return the re-grasp motion to connect  $q_s$  to  $q_t$  (line 10).

## C. Sampling stable intersections of grasp manifolds

A grasp path provides necessary but not sufficient conditions of the connectivity of their corresponding grasp manifolds. To check this connectivity, given two subsequent grasps  $g$  and  $g'$ , we need to identify configurations at which both grasps are feasible and stable against gravity. Particularly in our task, given the transition from a bimanual grasp to a unimanual grasp, the object may not be stable against the gravity and slide within the remaining gripper. Fig. 1(b) shows one such configuration in the bottom right corner which is not stable and a configuration, where the same transition is stable due to a good choice of the configuration. Such configurations correspond to the intersections of the two grasp manifolds that are stable against gravity.

In Alg. 1, the procedure *SampleIntersection* samples  $m$  such configurations. To generate one such configuration, we first sample an object pose in the reachable space of the robot (line 4). Then, we solve the inverse-kinematics for the bimanual grasp at the sampled object pose, giving us a configuration  $q$  (line 5). We check (line 6) whether both grasps  $g$  and  $g'$  are stable against gravity at  $q$ , using the same stability check described in Sec. III-A.1. A stable configuration  $q$  is returned as a candidate point connection in the final solution path (line 7).

#### D. Connectivity of sequence of manifold intersections

Given two configurations  $q_s$  and  $q_t$ , and stable configurations sampled at the intersections of a sequence of manifolds (i.e., the manifolds of the grasp sequence  $G$ ), we search for motion plans that connect  $q_s$  to  $q_t$  through these manifolds.

In Alg. 1, the procedure *Connect* implements this process as depth-first-search. Given a current configuration  $q_s$  and a sequence of grasps  $G = (g_1, g_2, \dots, g_n)$  (where  $g_1$  is the grasp in  $q_s$ ), we sample the intersection of the first two grasps in the sequence for stable configurations (line 7). We then try to plan a motion from  $q_s$  to a sampled configuration  $q$  (line 9). Note that this is a motion plan within a single manifold (the manifold of grasp  $g_1$ ) and can be generated by existing closed-chain or single-arm motion planners. These paths, however, must also be stable against gravity, for which constrained motion planners [23], [24] can be used. If the motion plan is successful, the trajectory is returned along with a recursive call to the depth-first-search. Lines 1-6 handle the simple case where  $q_s$  and  $q_t$  are already on the same manifold.

## IV. EXPERIMENTS AND RESULTS

In this section, we present experiments to verify the performance of the proposed planners in terms of minimizing the number of regrasps and planning stable regrasps efficiently. The planners are applied to Baxter developed by Rethink Robotics in an OpenRAVE environment [25]. Baxter has two 7-DOF manipulators, each equipped with a parallel jaw gripper. We used a modified BiRRT planner [26] as implemented in OpenRAVE as the motion planner to connect two configurations.

The planners were tested on two types of forceful operations on a board, *drilling* and *cutting*. For all the drilling operations, we randomly changed the magnitude of the drilling forces from  $10\text{ N}$  to  $15\text{ N}$  and we assume the forces are normal to the surface of the board. For the cutting forces, we assume their magnitude varies between  $30\text{ N}$  to  $60\text{ N}$ . These operations are instantiated into three categories of tasks, including:

- *random-drilling*: Each task contains 10 drilling operations randomly distributed on the surface of the board. An example is shown in Fig. 6;
- *tick-drilling*: Each task contains 40 drilling operations along two random line segments meeting at a common point. An example is shown in Fig. 8;

TABLE I  
NUMBERS OF REGRASPS (WITH STANDARD DEVIATIONS) OF THREE PLANNERS ON THREE DIFFERENT TASKS.

	Random-drilling	Tick-drilling	Drilling&cutting
Random	17.6(0.9)	48.7(10.7)	5.8(2.1)
Greedy	7.8(1.9)	4.3(2.4)	3.1(0.8)
Min-regrasp	5.2(0.9)	1.3(1.0)	2.0(0.0)

- *drilling&cutting*: Each example contains four drilling operations and a cutting operation as shown in Fig. 11.

We generate 100 random tasks for each category above.

In our experiments, we used a rigid foam board as the object. We also measured the force and torque limits (as explained in Sec. III-A.1) of the Baxter grippers on this object. Along each axis shown in Fig. 3, we applied increasing amount of forces and torques to find the point when the object started to slide between the parallel plates or when the object rotated more than  $5^\circ$  due to finger link deformation. We found the limits to be  $[P_x, P_y, P_z, R_x, R_y, R_z] = [13\text{ N}, 40\text{ N}, 13\text{ N}, 0.3\text{ Nm}, 0.05\text{ Nm}, 0.1\text{ Nm}]$ . Along the negative  $P_z$  direction, the object rests against the palm, therefore we used a large force limit ( $100\text{ N}$ ) in the negative direction of  $P_z$  when we solved Eq. 1.

#### A. Minimizing the number of re-grasps

First, we compared the performance of our planners, *min-regrasp* and *greedy*, with a random planner on the number of regrasps. The *random planner* acts as a baseline approach. For the first external force, the random planner samples a random configuration in the configuration space until it finds a feasible one. For any subsequent force, it first checks whether the configuration for the preceding force is still stable. If not, it falls back to random sampling.

Table I shows the average results of the three planners on 100 random task instances. For the random-drilling tasks, the random planner generates almost one bimanual regrasp for every external force (maximum 18 regrasps for 10 external forces). The min-regrasp does dramatically minimize the number of regrasps (5 regrasps for 10 external forces, an example solution is shown in Fig. 6). The greedy planner also performs well in terms of reducing regrasps (8 regrasps).

Similarly, for the tick-drilling tasks, the random planner generates plans with a large number of regrasps (49 regrasps for 40 external forces of each tick-drilling task), while min-regrasp planner just needs 1.3 regrasps (an example solution is shown in Fig. 8) and 2 regrasps for the drilling&cutting tasks on average. The greedy planner shows a much better performance compared with the random planner, but still worse than the min-regrasp planner. For example, as shown in Fig. 7, the greedy planner requires the grippers to climb along the edges of the board up and down frequently to follow the movements of the external forces, while the min-regrasp planner comes up with a plan of just two regrasps in Fig. 8. We present a complete run of such a plan on the real robot in the attached video.

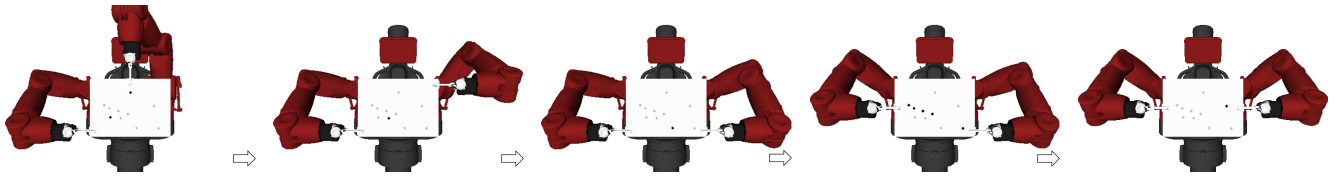


Fig. 6. A plan by the min-regrasp planner for a random-drilling task. The dark points indicate the drilling operations applied during the current grasp.

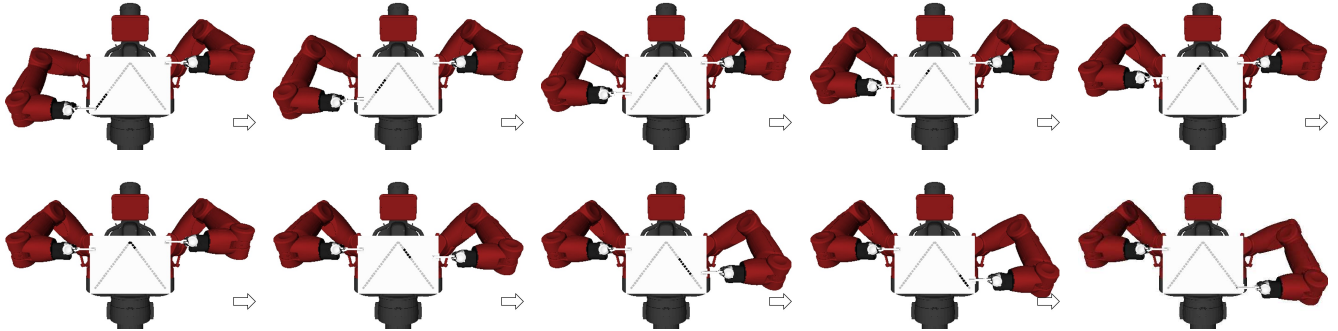


Fig. 7. A plan by the greedy planner for a tick-drilling task. The dark points indicate the drilling operations applied during the current grasp.

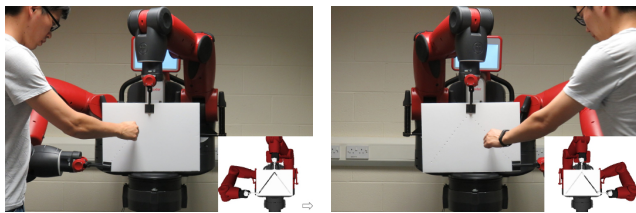


Fig. 8. A plan by the min-regrasp planner for a tick-drilling task.

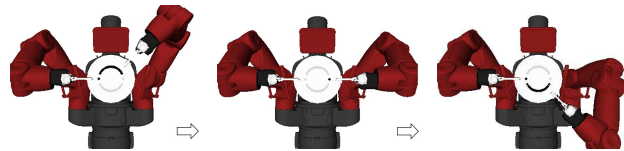


Fig. 9. A plan by the min-regrasp planner for drilling on a circular board.

We also counted the number of samples the random planner needed before it found a feasible grasp. On average, the random planner needed **35.8 samples** for each external force of the tasks above, showing that planning is necessary and random grasps have little chance of being feasible. Our planners are not limited to grasping rectangular objects. To demonstrate this, we tested the min-regrasp planner on a circular board with a sequence of 40 circular drilling operations. A plan with only two regrasps is shown in Fig. 9.

### B. Planning performance

We tested the performance of our planner on *light* and *heavy* objects respectively. We ran the planner on 100 randomly generated tasks for each category as discussed above. Table II shows the average planning time each layer of the planner takes, including time for generating stable

sequences (StabSeq for short in Table II), time for generating and searching the grasp graph combined with sampling intersections (SamPlnt, for short) and motion planning (Connect, for short). As the table shows, most time is spent on motion planning, while the time for planning stable configuration sequence and sampling intersection is negligible (The planner is set to generate a set of 20 feasible samples for each intersection). Planning for the heavy object takes significantly long time because finding stable regrasping configurations for this object is more difficult.

Fig. 10 shows an example regrasp sequence to regrasp a heavy object. For a light object, the robot can stably grasp and move the object using just a single gripper at most reachable configurations. Thus, mostly, the robot can directly release off and regrasp the object, without the need of reorienting it to intermediate configurations. However, for a heavy object, as discussed in Sec. I, the object may slip down between gripper fingers if the robot directly releases one gripper. That is, the robot needs to move it to intermediate configurations at which one single gripper is enough to keep the object stable. In Fig. 10, the robot first transfers the object to configurations in Fig. 10(b) and 10(d) before releasing one gripper. After releasing, most object weight will be resisted by the forces arising from gripper finger bending as shown in Fig. 10(c) and 10(e), which are much larger than the frictional forces between the object and finger surfaces.

### C. Real robot implementation

We ran our planner on a real Baxter robot for three tasks: cutting a circle, tick-drilling, and drilling&cutting tasks. The snapshots from these experiments are in Fig. 1, 8 and 11. The attached video (<https://youtu.be/IHti307yGFY>) also presents these experiments .

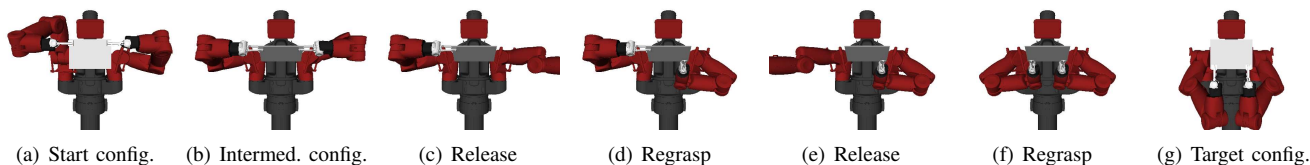


Fig. 10. Regrasping a heavy object.

TABLE II

PLANNING TIME FOR BOTH HEAVY AND LIGHT OBJECTS. TIMES ARE IN SECONDS. STANDARD DEVIATIONS ARE IN PARANtheses.

	random-drilling			tick-drilling			drilling&cutting		
	StabSeq	SampInt	Connect	StabSeq	SampInt	Connect	StabSeq	SampInt	Connect
heavy	11.2(2.5)	50.1(4.7)	440.0(62.3)	11.7(0.8)	12.8(1.0)	114.4(17.3)	2.2(0.2)	20.6(1.2)	139.1(25.0)
light	10.9(2.8)	17.8(1.9)	155.5(11.4)	11.9(0.8)	5.0(0.3)	39.8(8.3)	1.9(0.4)	6.6(0.7)	71(14.1)

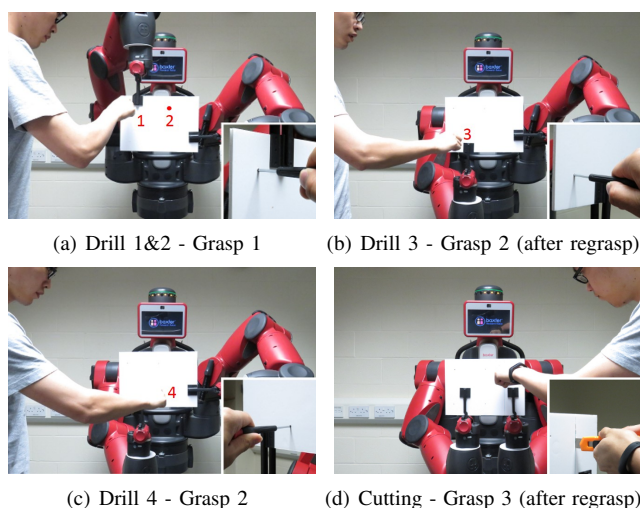


Fig. 11. Drilling&cutting task.

## V. CONCLUSION AND FUTURE WORK

We believe the planning system presented here can be a key component in a human-robot collaboration framework. In future work, we aim to include an increasing amount of human comfort factors (e.g. the human kinematics) in planning the collaboration between the human and the robot.

## REFERENCES

- [1] T. Siméon, J.-P. Laumond, J. Cortés, and A. Sahbani, “Manipulation planning with probabilistic roadmaps,” *IJRR*, 2004.
- [2] T. Lozano-Pérez, J. Jones, E. Mazer, P. O’Donnell, W. Grimson, P. Tournassoud, and A. Lanassee, “Handey: A robot system that recognizes, plans, and manipulates,” in *ICRA*, 1987.
- [3] P. Tournassoud, T. Lozano-Pérez, and E. Mazer, “Regrasping,” in *ICRA*, 1987.
- [4] W. Wan and K. Harada, “Developing and comparing single-arm and dual-arm regrasp,” *RA-L*, 2016.
- [5] —, “Integrated assembly and motion planning using regrasp graphs,” *Robotics and biomimetics*, vol. 3, no. 1, p. 18, 2016.
- [6] M. Dogar, A. Spielberg, S. Baker, and D. Rus, “Multi-robot grasp planning for sequential assembly operations,” in *ICRA*, 2015.
- [7] P. Lertkultanon and Q.-C. Pham, “A certified-complete bimanual manipulation planner,” *arXiv preprint arXiv:1705.02573*, 2017.
- [8] T. Bretl, “Motion planning of multi-limbed robots subject to equilibrium constraints: The free-climbing robot problem,” *IJRR*, 2006.
- [9] K. Kosuge and N. Kazamura, “Control of a robot handling an object in cooperation with a human,” in “*RO-MAN*”, 1997.
- [10] L. Rozo, S. Calinon, D. G. Caldwell, P. Jimenez, and C. Torras, “Learning physical collaborative robot behaviors from human demonstrations,” *IEEE Transactions on Robotics*, 2016.
- [11] F. Abi-Farraj, T. Osa, N. Pedemonte, J. Peters, G. Neumann, and P. G. Robuffo, “A learning-based shared control architecture for interactive task execution,” in *ICRA*, 2017.
- [12] R. Luo, R. Hayne, and D. Berenson, “Unsupervised early prediction of human reaching for human–robot collaboration in shared workspaces,” *Autonomous Robots*, pp. 1–18.
- [13] G. J. Maeda, G. Neumann, M. Ewerton, R. Lioutikov, O. Kroemer, and J. Peters, “Probabilistic movement primitives for coordination of multiple human–robot collaborative tasks,” *Autonomous Robots*, vol. 41, no. 3, pp. 593–612, 2017.
- [14] K. W. Strabala, M. K. Lee, A. D. Dragan, J. L. Forlizzi, S. Srinivasa, M. Cakmak, and V. Micelli, “Towards seamless human-robot handovers,” *Journal of Human-Robot Interaction*, vol. 2, no. 1, pp. 112–132, 2013.
- [15] A. T. Miller and P. K. Allen, “Graspit! a versatile simulator for robotic grasping,” *IEEE Robotics & Automation Magazine*, vol. 11, no. 4, pp. 110–122, 2004.
- [16] K. Hauser and J.-C. Latombe, “Multi-modal motion planning in non-expansive spaces,” *IJRR*, vol. 29, no. 7, pp. 897–915, 2010.
- [17] G. Lee, T. Lozano-Pérez, and L. P. Kaelbling, “Hierarchical planning for multi-contact non-prehensile manipulation,” in *IROS*, 2015.
- [18] M. Uchiyama and P. Dauchez, “A symmetric hybrid position/force control scheme for the coordination of two robots,” in *ICRA*, 1988.
- [19] —, “Symmetric kinematic formulation and non-master/slave coordinated control of two-arm robots,” *Advanced Robotics*, 1992.
- [20] B. Mishra, J. T. Schwartz, and M. Sharir, “On the existence and synthesis of multifinger positive grips,” *Algorithmica*, 1987.
- [21] C. Ferrari and J. Canny, “Planning optimal grasps,” in *ICRA*, 1992.
- [22] C. Borst, M. Fischer, and G. Hirzinger, “Grasp planning: How to choose a suitable task wrench space,” in *ICRA*, 2004.
- [23] D. Berenson, S. Srinivasa, and J. Kuffner, “Task space regions: A framework for pose-constrained manipulation planning,” *IJRR*, vol. 30, no. 12, pp. 1435–1460, 2011.
- [24] L. Jaillet and J. M. Porta, “Path planning under kinematic constraints by rapidly exploring manifolds,” *IEEE Transactions on Robotics*, vol. 29, no. 1, pp. 105–117, 2013.
- [25] R. Diankov and J. Kuffner, “Openrave: A planning architecture for autonomous robotics,” *Robotics Institute, Pittsburgh, PA, Tech. Rep. CMU-RI-TR-08-34*, vol. 79, 2008.
- [26] J. J. Kuffner and S. M. LaValle, “Rrt-connect: An efficient approach to single-query path planning,” in *ICRA*, 2000.